 CMES, vol.45, no.2, pp.155-177, 2009

An Integrated Finite Strip Solution for Box Girder Bridges and Slab-on-girder Bridges

Moe M. S. Cheung[1], **Zhenyuan Shen**[2] **and Ben Y.B. Chan**[3]

Abstract: In view of the urgent need for an efficient and accurate structural analysis method in bridge design practice, this paper introduces a total integrated analytical solution for multi-span, continuous slab-on-girder and box girder bridges, by modeling the bridge deck and the piers together, using the finite strip method (FSM). FSM has been well accredited for its efficiency in the structural analysis of bridges, reducing the time required for data input and analysis without affecting the degree of accuracy. By using a continuously differentiable smooth series in the longitudinal direction, a complex 3D problem is reduced to a 2D problem using the FSM. However, difficulties are encountered when components of different orientation, such as the piers, are included to the formulation. Thus, the analytical model developed using the conventional FSM is limited to the super-structures, without proper consideration of the interactions between the bridge deck (super-structure) and piers (sub-structure).

In this regard, a cantilever type of pier strip element is formulated by the authors, based on the spline finite strip concept, which is compatible with the well developed spline finite strip bridge deck. In addition, by combining the piers and the bridge deck altogether in a single finite strip formulation, with some appropriate connecting boundary conditions, the time required for both static and dynamic analysis can be significantly reduced.

In this paper, the development and verification of the vertical cantilever strip is introduced and the overall integrated method of analysis is presented with the aid of numerical examples. In addition, the efficiency of the proposed approach in seismic analysis using the Pseudo Excitation Method (PEM) is also demonstrated as an extension of its application.

[1] Department of Civil Engineering, The Hong Kong University of Science and Technology, Clear Water Bay, Kowloon, Hong Kong SAR, China. E-mail: mscheung@ust.hk , Phone; (852) 2358-8191, Fax: (852) 2358-1534

[2] Department of Civil Engineering, The Hong Kong University of Science and Technology, Clear Water Bay, Kowloon, Hong Kong SAR, China. E-mail: zhenyuan@ust.hk

[3] Department of Civil Engineering, The Hong Kong University of Science and Technology, Clear Water Bay, Kowloon, Hong Kong SAR, China. E-mail: ybchan@ust.hk

Keywords: Finite Strip Method, Pseudo Excitation Method, Dynamic Analysis, Box-girder Bridge.

1 Introduction

The quasi-static analysis approach in bridge design has been used for over a century. However, with the successful application of stiff and light-weight composite materials in recent years, the clear span length of bridges nowadays are increasing at a faster pace than ever. Consequently, the critical design criteria have shifted from the static ultimate and serviceability considerations to the dynamic driven failure mechanisms. It is becoming obvious that the dynamic characteristics of these structures have become significant and the conventional design approach is no longer appropriate. Nevertheless, the formulation of a FEM model and the setting up of boundary conditions of a three dimensional (3D) bridge for dynamic analysis is very complicated and time consuming, and this makes the dynamic analysis of long span bridges extremely difficult in real design process. Besides, the convergence rate of the conventional FEM in dynamic problems is usually slow, since the nonlinearities associated with the flexible bridge structures lead to a significant redistribution of internal forces. One of the solutions for improving the convergence rate is to use very small elements throughout the structure, resulting in a large number of degrees of freedom. Although, some extended techniques, such as the mesh-free approach [Dang and Sankar (2008) and Hagihara (2007)], have been developed recently to accelerate the FEM analysis, the difficulty for FEM to perform large-scale problem is still quite obvious. In this regard, two streams of technique were vigorously developed in recent years to reduce the computational demand: the Boundary Element Method (BEM) and the Finite Strip Method. The BEM takes advantage of the finite-part integrals to reduce the apparent dimension of the model. With its absolute generality and the extended solver developed in recent years [He et. al. (2008), Liu (2007), Owatsiriwong et. Al. (2008), etc.], the application of BEM has been extended to shell problems [Albaguergue and Aliabodi (2008)] and three-dimensional interface problems [Wang and Yao (2005, 2008)]. In addition, BEM has also been proven to be able to perform crack and fracture analysis [Zhou et. Al. (2008), Shiah and Tan (2000)]. However, the formulation for the BEM problem is still quite complicated and is usually applied together with the FEM [Liu and Yu (2008)].

On the other hand, FSM seems to have provided an ideal solution for bridge analysis, by reducing the input-output time requirement and the computational loading demand. Pioneered by Cheung [Cheung (1976), Cheung et. al. (1982)] and the first author [Cheung and Cheung (1970), (1971), (1972)], FSM is a well-known numerical method in structural analysis and has been well-recognized as one of

the most efficient tools for the analysis of bridge super-structures due to its semi-analytical nature as well as its pre-set boundary conditions [Cheung, Li and Chidiac (1996)]. Early versions of the FSM, devised in the 1960s, were restricted to regular prismatic structures only. However, the robustness of the approach attracted many bridge engineers to extend the application in the past few decades. Since the development of the B_3 spline function and spline finite strips by Prenter (1975), FSM has been extended for the analysis of more complex structures and problems. Among such problems are buckling and vibration analysis of composite laminated plates [Yuan and Dawe (2004)], nonlinear analysis of Mindlin plates, fracture problems [Cheung and Jiang (1996)] as well as the analysis of double curvature laminated shells and buckling of thin-walled shell structures [Cheung and Kong (1995)]. The semi-analytical FSM is effective in reducing the computational effort needed for relatively simple structures with regular geometries, and made of isotropic or orthotropic materials; while the Spline Finite Strip Method (SFSM) is efficient and flexible in handling structures with complex boundary conditions, anisotropic material properties, as well as complicated loading conditions. Wang and Zhang (2004) summarized the advantages and constraints of FSMs in a recent review. The FSM is an ideal approach for analyzing the dynamic properties of bridge deck structures, especially when dealing with slab-on-girder and box girder structures that have pre-set boundary conditions.

In spite of the large number of publications on the use of FSM in superstructure analysis, the application of the existing FSM in full-bridge analysis is limited. The FSM adopts a continuously differentiable smooth series in the longitudinal direction, and difficulties are encountered in combining different types of structural components in different directions. It is not possible to insert an extra component at an intermediate point within a strip, from the finite strip point of view. Therefore, the analytical model developed using the conventional finite strip method is limited to super-structures with the piers of the bridge replaced by some assumed boundary conditions. However, this assumption is limited to quasi-static analysis, in which only the stress distribution along the girders and slab of the bridge super-structures is required. Without physical piers being included in the finite strip model, the interactions between the bridge deck and the piers cannot be properly investigated. An alternative solution for considering the pier effect is to combine the finite strip bridge deck with piers modeled by other types of element, such as the boundary elements, and the interactions between the bridge deck and the piers can be obtained via an iterative process. Nevertheless, this approach is effective for simple structures under static/quasi-static loading only. When complicated structures or structures under dynamic excitation, such as non-uniform seismic analysis, are being considered, such simplification can no-longer be adopted. For instance, the

ground excitations are transmitted from the piers to the super-structure and the dynamic characteristics of the piers play an important role in the prediction of the bridge responses. It has also been demonstrated in several major earthquake events that many cases of seismic damage to bridges were caused by the excessive deformation of the piers.

In this paper, a general integrated framework is developed to solve the static and dynamic structural problems in an efficient and vigorous manner, under the FS environment. In order to achieve a full bridge model with high accuracy, the authors have reformulated the conventional spline finite strip element to describe the piers in a finite strip formulation and have developed an integrated procedure to connect the pier strips to the deck strips, considering the interactions between them. The details for the modeling of piers connecting to bridge super-structures in the FS formulation, including the development of the vertical-cantilever pier strips and the combination technique for strips in different orientation, are covered in the following sections. In addition, the efficiency and effectiveness of the approach is discussed using some real bridge numerical examples.

2 Formulation of the piers in finite strip environment

The original idea for the FSM was to reduce the dimensions of a long span structure via the implementation of an analytical solution along the longitudinal direction. Therefore, the formulation of the conventional strip elements is limited to some common boundary conditions for the bridge deck only. To provide a total solution for bridge analysis in the finite strip formulation, with consideration of the piers, a special type of strip element is derived from the principle of the finite strip concept. To maintain compatibility and uniqueness throughout the whole structure, the more general B_3 spline finite strip function in the longitudinal direction is adopted as the basis for the development of the cantilever pier strip's displacement field. In the transverse direction, a cubic polynomial is applied to represent the variation of the vertical displacement, whereas linear interpolation is adopted for the in-plane displacements. The B_3 spline function is a piecewise cubic polynomial with continuity over the entire interval up to the second derivative. For a conventional B_3 spline finite strip, in order to interpolate an arbitrary function $f(y)$ by the spline functions, $f(y)$ is divided into several sections, known as knots. For an equally spaced spline function $\Phi_m(y)$with the center at $y = y_m$, the B_3 spline function is

defined as [Prenter (1975)]:

$$\Phi_m(y)=\frac{1}{6h^3}\begin{cases}(y-y_{m-2})^3, & y_{m-2}\le y\le y_{m-1}\\ h^3+3h^2(y-y_{m-1})+3h(y-y_{m-1})^2-3(y-y_{m-1})^3, & y_{m-1}\le y\le y_m\\ h^3+3h^2(y_{m+1}-y)+3h(y_{m+1}-y)^2-3(y_{m+1}-y)^3, & y_m\le y\le y_{m+1}\\ (y_{m+2}-y)^3, & y_{m+1}\le y\le y_{m+2}\\ 0, \quad \text{otherwise}\end{cases} \tag{1}$$

in which h is the width of these equal sections.

The spline functions centered at all the knots comprise a series of functions that can be used to interpolate an arbitrary function, and the series can be expressed as:

$$f(y)=\sum_{m=-1}^{r+1} a_m\Phi_m(y) \tag{2}$$

in which the values of a_m are coefficients determined by the required boundary conditions.

The solution of each section is in connection with the four spline functions, which are the functions centered at the two ends of the section and the two knots next to those ends, respectively. Thus, two additional knots are needed to complete the interpolation of the whole function. For a strip divided into r sections, $r+3B_3$ spline functions are needed.

In the formulation of SFSM, it is better to have the location of the supports and the concentrated load coinciding with the knots on the nodal lines, in order to obtain satisfactory results. Therefore, in the case of unequally spaced knots being adopted, the spline function centered at y_m can be expressed as:

$$\Phi_m(y)=\begin{cases}0 & y<y_{m-2}\\ f_1 & y_{m-2}\le y<y_{m-1}\\ f_2 & y_{m-1}\le y<y_m\\ f_3 & y_m\le y<y_{m+1}\\ f_4 & y_{m+1}\le y<y_{m+2}\\ 0 & y_{m+2}\le y\end{cases} \tag{3}$$

where

$$
\begin{aligned}
f_1 &= \frac{(y-y_{m-2})^3}{(y_{m+1}-y_{m-2})(y_m-y_{m-2})(y_{m-1}-y_{m-2})} \\
f_2 &= f_1 - \frac{(y_{m+2}-y_{m-2})(y-y_{m-1})^3}{(y_{m+2}-y_{m-1})(y_{m+1}-y_{m-1})(y_m-y_{m-1})(y_{m-1}-y_{m-2})} \\
f_3 &= f_4 - \frac{(y_{m+2}-y_{m-2})(y_{m+1}-y)^3}{(y_{m+1}-y_{m-2})(y_{m+1}-y_{m-1})(y_{m+1}-y_m)(y_{m+2}-y_{m+1})} \\
f_4 &= \frac{(y_{m+2}-y)^3}{(y_{m+2}-y_{m-1})(y_{m+2}-y_m)(y_{m+2}-y_{m+1})}
\end{aligned}
\tag{4}
$$

Considering the situation with the bridge deck resisting in-plan stresses and bending, the flat shell spline finite strip [Cheung and Fan (1983)] is chosen to model the deck, as shown in Fig. 1. For each knot, four degrees of freedom, three translational degrees-of-freedom (u, v, w) and one rotational degree-of-freedom ($\theta = dw/dx$), were assigned respectively.

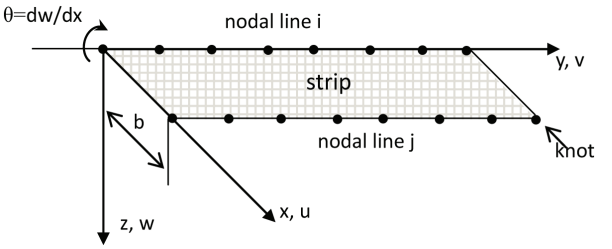

Figure 1: Flat shell spline finite strip

Defining x, y and z as the transverse, longitudinal and vertical directions of the shell strip, respectively, the corresponding displacements u, v and w were chosen, to satisfy the preset boundary conditions [Cheung and Li (1990); Cheung, Li and Jaeger (1992)]:

$$U = \sum_{m=-1}^{+1} \left((1-X)u_{im} + Xu_{jm} \right) \Phi_m(y)$$

$$V = \sum_{m=-1}^{+1} \left((1-X)v_{im} + Xv_{jm} \right) \Phi_m(y)$$

$$W = \sum_{m=-1}^{+1} \left((1-3X^2+2X^3)w_{im} + x(1-2X+X^2)\theta_{im} + (3X^2-2X^3)w_{jm} + x(X^2-X)\theta_{jm} \right) \Phi_m(y)$$

(5)

where $X = x/b$, b is the width of the strip; r is the total number of longitudinal sections on a nodal line; u_{im}, v_{im}, w_{im} and θ_{im} are the displacement parameters of the knot m on nodal line i; $\Phi_m(y)$ is the B_3 spline function centered at y_m.

As shown in Eq. 5, the in-plane displacements u and v are modeled by linear functions in the transverse direction, while the spline functions are assigned in the longitudinal direction. Similarly, the bending displacements and shapes are modeled by a cubic Hermite polynomials in the transverse direction and by spline functions in the longitudinal direction. The formulation procedure for the pier strip is similar to the conventional spline finite strip.

To develop a strip for the formulation of the piers, it is necessary to start by achieving a continuous shape function which satisfies the bending behavior and the boundary conditions for a cantilever-behaved pier. Consider a vertical cantilever strip, fixed at one end while leaving the other end free, as shown in Fig. 2.

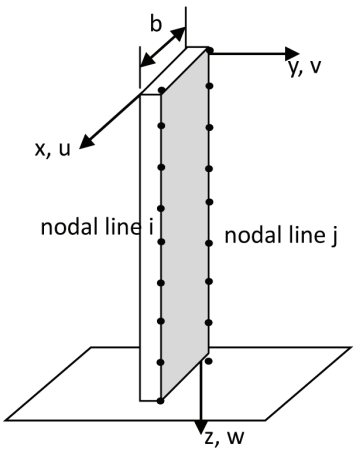

Figure 2: Vertical cantilever strip element

The global z-direction of the column strip is similar to the local v-direction in the conventional spline finite strip, and is controlled by the in-plane stiffness in the corresponding direction. Similarly, the global v-direction of the column strip is similar to the local z-direction of the conventional spline finite strip. According to the above information, the displacement function for the column strip can be

expressed as:

$$U = \sum_{m=1}^{r+1} \left((1-X) u_{im} + X u_{jm} \right) \Phi_m(y)$$
$$V = \sum_{m=1}^{r+1} \left(\left(1-3X^2+2X^3\right) v_{im} + x\left(1-2X+X^2\right) \varphi_{im} + \left(3X^2-2X^3\right) v_{jm} + x\left(X^2-X\right) \varphi_{jm} \right) \Phi_m(z)$$
$$W = \sum_{m=1}^{r+1} \left((1-X) w_{im} + X w_{jm} \right) \Phi_m(z) \tag{6}$$

With the assumed displacement functions and the preset boundary conditions, the shape function of the column strip, N, can be developed using the traditional finite element concepts. It should be noted that all strip elements in the finite strip method must come with the preset boundary conditions. Therefore, the strip developed for the piers must satisfy the fixed-free boundary condition, as for a vertical cantilever. Once the shape function is defined, the stiffness matrix ($[K_c]$) and the mass matrix ($[M_c]$) of the vertical-cantilever pier strip can be calculated using the following equations:

$$[M_c]_{mn} = \int \rho h [N]_m^T [N]_n \, dA \tag{7}$$

$$[K_c]_{mn} = \int [B]_m^T [D] [B]_n \, dA \tag{8}$$

in which ρ is the density of the strip and h is the thickness of the strip; [D] and [B] are the elastic matrix and the strain matrix respectively; [N] is the shape function matrix.

3 Parametric study of the pier modeled by FSM

To investigate the accuracy of the proposed pier model, a full parametric study has been performed. The study tried to look at the accuracy of the finite strip pier, compared with the FEM solution, for columns with different dimensions and different loading combinations. Concrete columns of different dimension ratios (height [h]: width of strip [b]: strip thickness [t]) were investigated, with h ranging from 5m to 30m, while both b and t ranged from 0.5m to 3 m, respectively. To investigate the top deflection of the columns in different directions, five different load cases were considered, including the combined effect of axial and bending forces, as shown in Fig. 3. For the FEM solutions, models were constructed in SAP2000 using general shell elements for b/t ratios larger than 1.5 or frame elements for b/t ratios less than

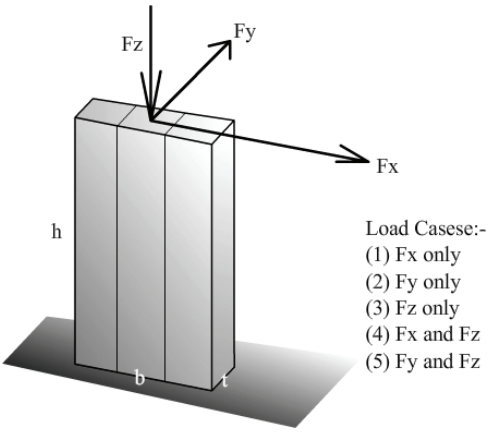

Figure 3: Column Strip – configuration for parametric study

1.5. Besides, the FEM models were finely meshed in all directions to achieve a more accurate result.

The result of the parametric study demonstrated that the finite strip columns can accurately model all types of column behaved pier structures for all loading conditions except load case number 5. In general, the difference increases as the height of the column decreases, but the absolute difference between the two methods is less that 2% in all trials. On the other hand, the percentage error for a combination of axial load and lateral load in the x-direction (load case number 5 with combined axial and lateral actions), as shown in table 1, suggests that the proposed strip is still capable of modeling the deflection for most columns. However, as the column becomes extremely short, with a very large sectional area, the percentage difference between the FSM and the FEM solution increases. When a very stiff short column under axial and bending forces is being considered, the deflection is highly restrained and influenced by the boundary condition and the preset shape function of the cantilever strip cannot accurately represent the actual deflection behavior in such a case. Nevertheless, a pier with height less than 6m and having a sectional area larger than $6m^2$ is relatively unlikely in reality.

4 Deck-pier connectivity

As discussed in the previous sections, the beauty of the FSM is the ability to reduce a 3D problem into a sectional 2D problem by introducing an analytical solution in the longitudinal direction. In the longitudinal direction, a strip is ideally defined by the preset boundary conditions at the two ends and some intermediate knots

Table 1: Difference in top drift between FEM and FSM for columns (Axial+Lateral)

Col. Size (m)			% Diff.	Col. Size (m)			% Diff.
b	t	h		b	t	h	
0.5	0.5	5	**1.143**	3	0.5	5	**1.892**
0.5	0.5	5.5	**1.000**	3	0.5	5.5	**1.746**
0.5	0.5	6	**0.887**	3	0.5	6	**1.108**
0.5	0.5	7	**0.728**	3	0.5	7	**0.597**
0.5	0.5	8	**0.620**	3	0.5	8	**0.237**
0.5	0.5	10	**0.486**	3	0.5	10	**0.159**
0.5	0.5	15	**0.345**	3	0.5	15	**0.476**
0.5	0.5	30	**0.253**	3	0.5	30	**0.438**
0.5	1	5	**0.375**	3	1	5	**0.300**
0.5	1	5.5	**0.383**	3	1	5.5	**0.277**
0.5	1	6	**0.398**	3	1	6	**0.522**
0.5	1	7	**0.394**	3	1	7	**0.507**
0.5	1	8	**0.407**	3	1	8	**0.907**
0.5	1	10	**0.419**	3	1	10	**0.687**
0.5	1	15	**0.444**	3	1	15	**0.717**
0.5	1	30	**0.450**	3	1	30	**0.499**
0.5	3	5	**0.767**	3	3	5	**23.095**
0.5	3	5.5	**0.717**	3	3	5.5	**20.452**
0.5	3	6	**0.750**	3	3	6	**15.278**
0.5	3	7	**0.460**	3	3	7	**12.267**
0.5	3	8	**0.619**	3	3	8	**4.124**
0.5	3	10	**0.370**	3	3	10	**6.289**
0.5	3	15	**0.437**	3	3	15	**3.368**
0.5	3	30	**0.454**	3	3	30	**1.131**

only. The physical properties in the longitudinal direction of the strip are modeled by continuously smooth functions and the concept of elements or nodes dose not exist. Thus, without the nodal concept, the piers and the superstructure cannot be connected under the conventional finite strip formulation, and this is becoming the major obstacle for the application of FSM in real practice. Although the the FSM has been widely recognized as an efficient tool in structural analysis, it is still limited to a narrow range of applications, without an effective approach for combining strips with different orientations in a single finite strip formulation.

Under the concept of the spline finite strip, there are some pre-defined continuously smooth functions in the longitudinal direction, and the knots available within the strips are points for spline interpolation only. Unlike the nodal definition in FEM, the properties of each knot in SFSM is a function of the properties of surrounding knots , and a minimum of 2 extra knots is required to define the properties of a particular knot. Although it is impossible to connect an extra element to a particular knot, it is made possible by introducing a tiny rigid element to connect two knots in each strip for force and displacement transfer.

Fig. 4 demonstrates a typical cross-shaped transition section, defined in such a way that h is much smaller than H. By connecting two knots on each side, the displacement of the internal knots within the rigid transition section can be defined. Thus, compatibility for the displacements of the deck and pier is achieved, and the integrated system of the spline finite strip model can be constructed. Depending on the structure complexity, one may choose different values of h to meet the required accuracy. The numerical study shows that, in most of the cases, h/H=0.001 is good enough to achieve an acceptable tolerance of error (less than 0.5%), for engineering analysis.

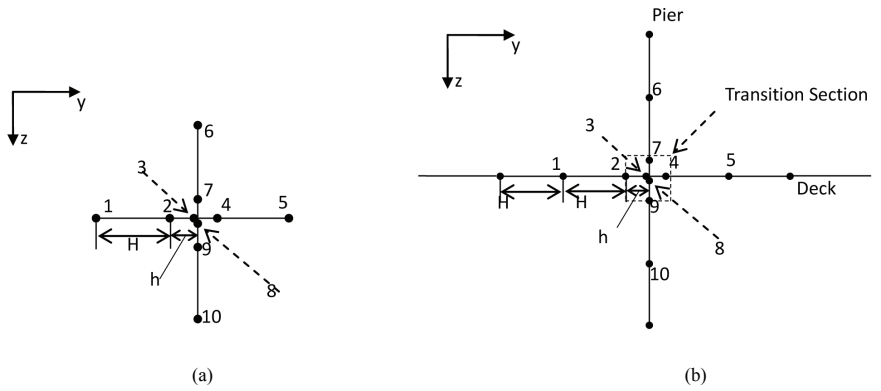

Figure 4: (a) Typical transition section; (b) Transition section between Deck and Pier

5 Accuracy of the finite strip full bridge model

To verify the accuracy and efficiency of the proposed integrated finite strip solution, a concrete slab bridge model, as shown in Fig. 5, is presented here. The modulus of elasticity $E = 3.0 \times 10^4$MPa, Poisson's ratio is 0.2 and the material density is 2500 kg/m^3. Both SFSM and FEM are adopted to model the static and dynamic

behavior of the structure, and the results from the different methods are compared.

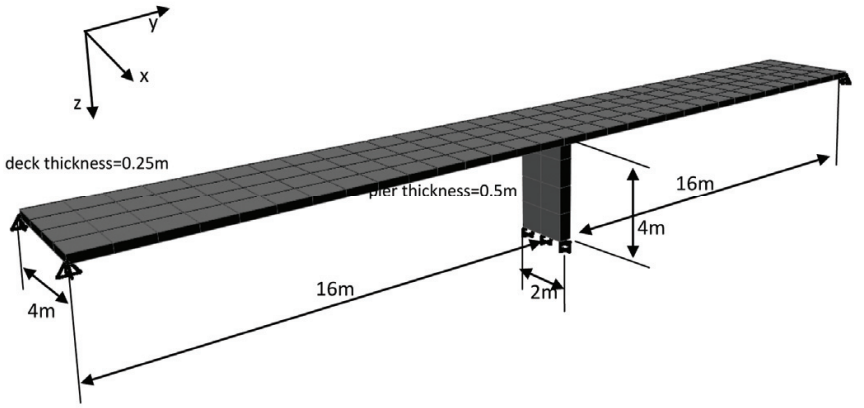

Figure 5: A Simple Slab Bridge: (a) 3D bridge model; (b) SFSM Model.

5.1 Accuracy

Three numerical methods were adopted to model the static behavior of the structure, the proposed integrated SFS model with piers, the coarsely meshed FE model and the finely meshed FE model.

For the integrated SFS model, a FS full bridge model is constructed, using B_3 spline finite strip for the deck, vertical-cantilever strip for the piers and transition elements for the bearings, as illustrated in the previous sections. The deck is divided into four equal strips, while the pier is divided into two cantilever strips. Each deck strip is composed of 32 sections as well as two additional transition sections. Each pier strip is composed of 4 sections, as well as one transition section. For the coarsely meshed FE model, the mass and stiffness of the bridges is constructed with five degrees-of-freedom shell elements throughout the structure. The shell element is derived from a combination of an in-plane element with translation in the local x and y directions, and a bending element with translation is the local z direction, plus bending above the local x and y directions. The deck is meshed with 32 by 4 elements, and the pier is meshed with 4 by 2 elements. For the finely meshed FE model, which is an indicator for a more accurate solution, finely meshed standard shell elements are employed to construct the model, with six degrees-of-freedom at each node.

For the static analysis, the ability of the transition element to transfer loading between the deck strip and the CS is assessed. Four load cases, with constant 1000kN

point forces acting on different structure components and in different directions, were assigned to the models as shown in Fig. 5b. The vertical and horizontal drifts along different nodal lines, determined from the three numerical methods, are summarized in tables 2 to 5. It is seen that the displacements calculated from the integrated approach agree well with the FEM results for all loading conditions, which indicates that the proposed approach can successfully model a full bridge structure in the finite strip environment, taking the pier-bearing-deck interaction into consideration. Besides, it can be observed from the static analysis result that the displacement determined from the integrated method is in better agreement with the finely meshed FE model. It is suggested that, even with similar node definitions as the coarsely mesh FE model, the proposed integrated approach generates a more accurate result than the FE method.

Table 2: Load Case (a)

deck: nodal line 3						
y (m)	translation: v (m)			translation: w (m)		
	Integrated SFSM	FEM Coarse mesh	FEM Refined Mesh	Integrated SFSM	FEM Coarse mesh	FEM Refined Mesh
0 (left)	0.00006522	0.00005738	0.00006300	-0.00079888	-0.00072660	-0.00075700
8	0.00012497	0.00011743	0.00012300	-0.15301200	-0.15287000	-0.15288800
16	0.00020521	0.00019624	0.00020300	0.00010095	0.00009521	0.00009500
24	0.00034266	0.00034280	0.00035500	0.38845500	0.38788000	0.38801600
32 (right)	0.00014974	0.00013522	0.00014500	0.00354105	0.00322160	0.00335200
pier: nodal line 7						
z (m)	translation: v (m)			translation: w (m)		
	Integrated SFSM	FEM Coarse mesh	FEM Refined Mesh	Integrated SFSM	FEM Coarse mesh	FEM Refined Mesh
0 (top)	0.00020521	0.00019624	0.00020300	0.00010093	0.00009521	0.00009500
2	0.00006644	0.00006174	0.00006400	0.00004560	0.00004532	0.00004500

5.2 Efficiency

Taking advantage of the reduced matrix size in a finite strip formulation, the proposed integrated approach can significantly reduce the computational effort demand. The above computations were executed on a typical personal computer with an Intel Core2 Duo CPU (1.66 GHz) and 3GB physical memory. The computer times required by different methods are compared in table 6. It is clear that the SFSM is more efficient and saves about 10% of the computer time. Considering it is only the static analysis, the proposed SFSM will save even more time for complicated dynamic analysis. Moreover, in order to achieve matching preconditions for

Table 3: Load Case (b)

deck: nodal line 3			
y (m)	translation: u (m)		
	Integrated SFSM	FEM Coarse mesh	FEM Refined Mesh
0 (left)	-0.00002077	-0.00001018	-0.00001600
8	0.00086462	0.00079028	0.00085600
16 (middle)	0.00169547	0.00155190	0.00167100
pier: nodal line 7			
z (m)	translation: u (m)		
	Integrated SFSM	FEM Coarse mesh	FEM Refined Mesh
0 (top)	0.00169549	0.00155190	0.00167100
2	0.00055785	0.00051387	0.00054800

Table 4: Load Case (c)

deck: nodal line 4			
y (m)	translation: w (m)		
	Integrated SFSM	FEM Coarse mesh	FEM Refined Mesh
0 (left)	0.00000005	0.00000005	0.00000005
8	0.00011698	0.00011110	0.00011700
16 (middle)	0.00020319	0.00019112	0.00020200
pier: nodal line 8			
z (m)	translation: w (m)		
	Integrated SFSM	FEM Coarse mesh	FEM Refined Mesh
0 (top)	0.00020320	0.00019112	0.00020200
2	0.00022347	0.00022282	0.00024000

analysis, similar meshes are chosen in the SFSM and the FEM models. However, due to its semi-analytical property in the longitudinal direction, the number of sections for each strip in the SFSM model can be significantly reduced without losing accuracy. Then the time for computation could be reduced, and greater efficiency could be achieved.

6 Integrated Solution for Dynamics

In order to optimize the advantages of the integrated finite strip solution, in terms of precision and efficiency, the authors adopted the Pseudo Excitation Method

Table 5: Load Case (d)

deck: nodal line 2			
y (m)	translation: v (m)		
	Integrated SFSM	FEM Coarse mesh	FEM Refined Mesh
0 (left)	0.00002773	0.00002350	0.00002600
8	0.00006233	0.00005756	0.00005900
16 (middle)	0.00014901	0.00013984	0.00014400
pier: nodal line 6			
z (m)	translation: v (m)		
	Integrated SFSM	FEM Coarse mesh	FEM Refined Mesh
0 (top)	0.00014904	0.00013984	0.00014400
2	0.00183751	0.00168860	0.00174300

Table 6: Computational time

Method	SFSM	Coarsely Meshed FEM
Computer time required for static analysis	4.717s	5.296s

(PEM) for the dynamic analysis to obtain the response probability spectrum density (PSD) of the structure. The recently developed PEM is an accurate and highly efficient dynamic analysis alternative for long-span structures [Lin (1992); Lin, Sun, D.K., Sun, Y. and Williams (1997); Lin, Zhang and Li (2004); Zhang, Li, Lin and Williams (2009)]. PEM is a modified response-spectrum method which has demonstrated its high efficiency by considering less than 300 modes, making the dynamic analysis process possible on a standard personal computer. Besides, the PEM has been successfully applied to many practical engineering analyses and has been proven to be effective and able to handle the seismic wave-passage effect in long-span bridges.

With the characteristic property matrices well defined in the FS environment, the conventional characteristic equation of motion can be constructed, and the dynamic analysis procedure, using the same approach as for FEM, can be applied.

The dynamic motion equation of a discrete structure can be written as:

$$[M]\{\ddot{u}\} + [C]\{\dot{u}\} + [K]\{u\} = \{p\} \tag{9}$$

where *{u}* is the relative displacement vector and *{p}* is the external force vector.

When the structure is subjected to uniform earthquake excitations, Eq. 9 can be

modified as:

$$[M]\{\ddot{u}\}+[C]\{\dot{u}\}+[K]\{u\}=-[M]\{r\}\ddot{u}_g(t) \tag{10}$$

in which *{r}* is the vector indicating the DOFs, which is influenced by the ground motion. $\ddot{u}_g(t)$ is the ground acceleration record of the excitation event.

Replacing the real excitation by the pseudo excitation, Eq. 10 can be rewritten as:

$$[M]\{\ddot{u}\}+[C]\{\dot{u}\}+[K]\{u\}=-[M]\{r\}\sqrt{S_{\ddot{u}_g}(\omega)}e^{i\omega t} \tag{11}$$

in which $S_{\ddot{u}_g}(\omega)$ is the auto-PSD of the ground acceleration.

By applying the conventional response analysis method for multi-degree-of-freedom systems, the pseudo displacement parameters of SFSM can be computed by the following equation:

$$\{\tilde{u}(\omega,t)\}=\sum_{j=1}^{m}\gamma_j H_j\{\varphi\}_j\sqrt{S_{\ddot{u}_g}(\omega)}e^{i\omega t} \tag{12}$$

$$H_j=\frac{1}{\omega_j^2-\omega+2i\varsigma_j\omega_j\omega} \tag{13}$$

$$\gamma_j=-\{\varphi\}_j^T[M]\{r\} \tag{14}$$

Here, ω_j is the jth angular frequency associated with matrices M and K; $\{\varphi\}_j$ is the corresponding normalized mode; ζ_j is the jth damping ratio.

By substituting the pseudo displacement parameters into the displacement functions (Eq. 5 & Eq. 6), the pseudo displacement responses $\left\{\tilde{U}(\omega,t)\right\}$ are obtained.

Hence, the PSD matrix of the displacements can be computed from:

$$S_U(\omega)=\left\{\tilde{U}(\omega,t)\right\}^*\left\{\tilde{U}(\omega,t)\right\}^T \tag{15}$$

7 Numerical Examples

A typical three-span concrete box girder bridge model , as illustrated in Fig. 6, is constructed by the proposed approach for further analysis. The deck and piers are all modeled by four degrees-of-freedom B_3 spline finite strips and the CSs respectively. One transition section is adopted at each connection between the deck and the pier. For all the components, the modulus of elasticity is $E=3.0\times10^4$MPa, Poisson's ratio is 0.2, and the material density is 2500 kg/m^3.

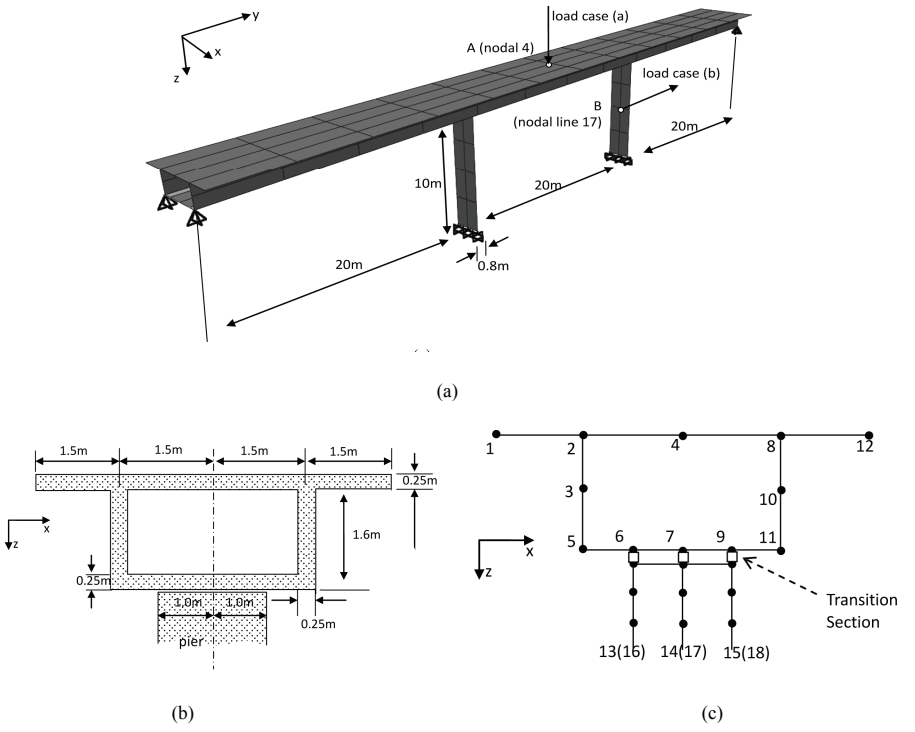

Figure 6: Three-span box girder bridge (a) 3D bridge model; (b) transverse cross-section through the pier and deck; (c) numerical model.

7.1 Static Analysis

In this part, two load cases with constant 1000kN point forces are assigned to the structure (see Fig. 6a). For the SFSM, each nodal line has 12 sections. For the FEM, two different meshes are adopted. One (tagged as FEM-1) uses the same mesh as the SFSM, which means that the top flange is divided into 12×4 elements. For the other mesh (tagged as FEM-2), the top flange is divided into 24×4 elements. The deflections along different directions from different methods are summarized in tables 7 and 8. It can be observed that the integrated finite strip solution is more accurate than FEM for the same mesh size in this model. It also indicates that for the analysis of bridges, especially for long-span bridges with complicated geometry, the proposed finite strip solution will be much more efficient than FEM when achieving the same precision.

Table 7: Load Case (a)

	deck: nodal line 4					pier: nodal line 14		
	y (m)	0 (left)	10	20	30(middle)	z (m)	0 (top)	5
w (m)	SFSM	-0.000006	-0.001210	0.000812	0.008293	SFSM	0.000190	0.000121
	FEM-1	-0.000015	-0.001250	0.000556	0.007121	FEM-1	0.000194	0.000111
	FEM-2	-0.000008	-0.001112	0.000794	0.008609	FEM-2	0.000189	0.000110

Table 8: Load Case (b)

	deck: nodal line 4						pier: nodal line 17		
	y (m)	0 (left)	20	30	40	60(right)	z (m)	0 (top)	5
v (m)	SFSM	0.000065	0.000107	0.000137	0.000131	0.000127	SFSM	0.000229	0.007096
	FEM-1	0.000064	0.000107	0.000137	0.000132	0.000127	FEM-1	0.000228	0.007358
	FEM-2	0.000067	0.000109	0.000138	0.000133	0.000129	FEM-2	0.000231	0.007359

7.2 Dynamic Analysis

The free vibration frequencies are extracted prior to the dynamic analysis and the first few natural frequencies from SFSM and FEM are given in table 9.

In this analysis, multiple support excitations, including the wave passage effect, are considered. An artificial seismic wave, illustrated in Fig. 7, is selected with the acceleration record acting in the transverse direction. The velocity of the seismic wave along the longitudinal direction is assumed to be 100m/s.

The PSD curves of the displacement responses of selected points on the deck and pier (see Fig. 6a) are illustrated in Fig. 8. Since PSD indicates the magnitude of the energy, as a function of frequency, it can be observed that these curves capture the characteristics of the structure response under the described seismic wave, which include the peaks of the first few natural frequencies and the drop of energy after about 10 Hz. The overall PSD curve of the pier is lower than that of the deck; however, the dynamic response of the pier can be quite critical at some frequencies. Moreover, for normal bridges, the piers are often stiffer than the deck, and the piers are more likely to be damaged during an earthquake. That is the reason why the pier must be considered in the dynamic analysis and has lead to the integrated finite strip solution being developed.

Table 9: Natural Frequency of Box Girder Bridge

Mode Number	Frequency		Mode Shape
	SFSM	FEM-2	
1	4.4973	4.2073	Sway (deck) symmetrical
2	8.8128	9.1936	Sway (deck) antisymmetrical
3	9.3038	9.3387	Heave (deck) symmetrical
4	9.6399	9.5630	Heave (deck) antisymmetrical
5	12.4600	11.9040	Heave (deck) symmetrical
6	18.8880	18.6550	Bending (pier) symmetrical
7	19.6140	19.2880	Bending (pier) antisymmetrical
8	20.9200	21.1790	Bending (pier) symmetrical + Sway (deck) antisymmetrical

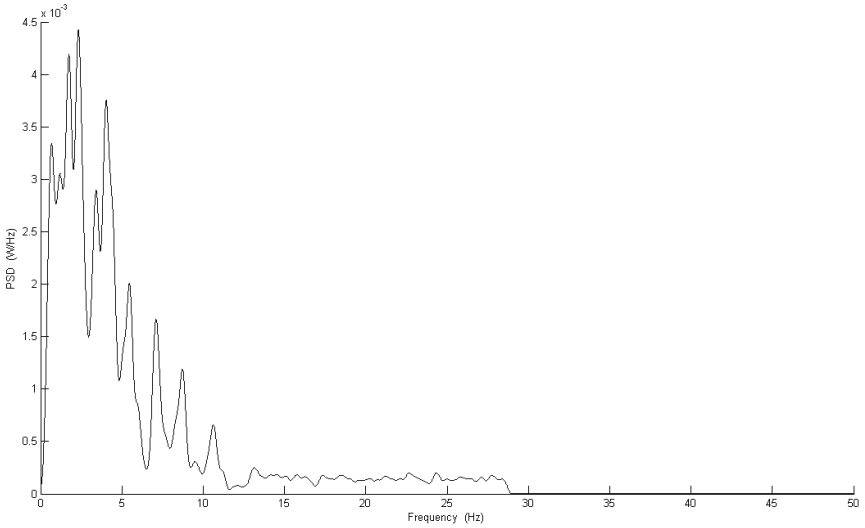

Figure 7: PSD of acceleration

8 Conclusion

This study has introduced a framework for constructing a full bridge model in the finite strip environment, by formulating a new type of strip element for the mod-

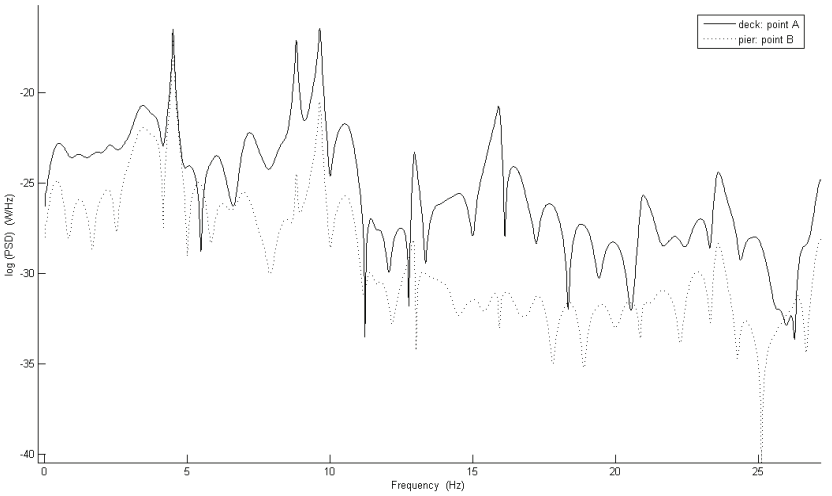

Figure 8: PSD of displacement response in transverse direction

eling of piers, and developing a special transition section to combine strips of different orientation. The piers modeled by the proposed finite strip method precisely describe the bending behavior of the pier structures in a spline finite strip environment. In addition, the full bridge model, constructed by combining the pier strip and the deck strip in a single finite strip formulation, can significantly reduce the input-output procedures and the computational effort required for both static and dynamic analysis. In this paper, the accuracy and efficiency of the proposed integrated finite strip solution has been demonstrated via two numerical examples

The strip combination technique introduced in this study has overcome the obstacles for the development of FSM. This has opened the door for complex dynamic analysis to be performed in the finite strip environment and has brought this efficient and effective method into a new era. Taken as a typical example for the extended application of the proposed approach, an innovative combination of the two very robust approaches, the proposed integrated finite strip method and the PEM, is introduced for seismic analysis.

Acknowledgement: The authors wish to gratefully acknowledge the financial support of the Hong Kong Research Grant Council RGC Reference Number 612106 for the finite strip analysis of the spatial vibration of multi-support, long span bridges.

References

Albuquerque, E. L.; Aliabadi, M. H. (2008): A boundary element formulation for boundary only analysis of thin shallow shells. *CMES: Computer Modeling in Engineering & Sciences*, vol. 29, no. 2, pp. 63-73.

Cheung M.S.; Cheung Y.K.; Ghali A. (1970): Analysis of Slab and Girder Bridges by the Finite Strip Method", *Building Science*, Vol. 5, no.2, pp. 95-104.

Cheung M.S.; Cheung Y.K. (1971): Analysis of Curved Box Girder Bridges by Finite Strip Method. *Publications IABSE,* vol. 31/I, pp.1-19.

Cheung M.S.; Cheung Y.K. (1972): Static and Dynamic Behaviour of Rectangular Plates Using Higher Order Finite Strips, *Building Science,* vol.7, no. 3, pp.151-158.

Cheung, M. S.; Li, W. (1990): Analysis of Haunched, Continuous Bridges by Spline Finite Strips. *Comput. Struct.*, 36(2), pp. 287-300.

Cheung, M. S.; Li, W.; Chidiac, S. E. (1996): *Finite strip analysis of bridges.* 1st Ed., E & FN Spon, London, New York.

Cheung, M. S.; Li, W.; Jaeger, L. G. (1992): Spline Finite Strip Analysis of Continuous Haunched Box-girder Bridges. *Can. J. Civil Eng.*, 19, pp. 724-728.

Cheung, Y. K.; Fan, S. C. (1983): Static analysis of right box girder bridges by spline finite strip method. *Proc. Inst. Civ. Eng.*, 2, 75, pp. 311-323.

Cheung, Y. K. (1976): Finite Strip Method in Structural Analysis. *Pergamon Press,Oxford, England*, 1976.

Cheung, Y. K.; Fan, S. C.; Wu, C. Q. (1982): Spline finite strip in structural analysis. *Proc. of Int. Conf. on Finite Element Method*, Shanghai, China, pp. 704-709.

Cheung, Y. K.; Jiang, C. P. (1996): Application of the finite strip method to plane fracture problems, *Engineering Fracture Mechanics*, vol 53, issue 1, pp. 89-96.

Cheung, Y. K.; Kong, J. (1995): Vibration and buckling of thin-Walled structures by a new finite strip, *Thin-Walled Structures*, vol 21, issue 4, pp. 327-343.

Fan, S.C.; Cheung, Y.K. (1983): Analysis of shallow shells by spline finite strip method, *Engineering Structures*, vol 5, issue 4, pp. 255-263.

Dang, T. D.; Sankar, B. V. (2008): Meshless local Petrov-Galerkin micromechanical analysis of periodic composites including shear loadings. *CMES: Computer Modeling in Engineering & Sciences*, vol. 26, no. 3, pp. 169–187.

Hagihara, S.; Tsunori, M.; Ikeda, T.; Miyazaki, N. (2007): Application of meshfree method to elastic-plastic fracture mechanics parameter analysis. *CMES: Computer Modeling in Engineering & Sciences*, vol. 17, no. 2, pp. 63–72.

He, X.F.; Lim, K.M.; Lim, S.L. (2008): Fast BEM solvers for 3D soisson-type equations. *CMES: Computer Modeling in Engineering & Sciences*, vol. 35, no. 1, pp. 21-48.

Lin, J. H. (1992): A Fast CQC Algorithm of PSD Matrices for Random Seismic Responses. *Comput. Struct.,* 44, pp. 683-687.

Lin, J. H.; Sun, D. K.; Sun, Y.; Williams, F. W. (1997): Structural Responses to Non-uniformly Modulated Evolutionary Random Seismic Excitations. *Commun. Numer. Meth. Eng.*, 13, pp. 605-616.

Lin, J. H.; Zhang, Y. H.; Li, Q. S. (2004): Seismic Spatial Effects for Long-span Bridges, Using the Pseudo Excitation Method. *Engineering Structure*, 26, pp.1207-1216.

Liu, C.S. (2007): A highly accurate solver for the mixed-boundary potential problem and singular problem in arbitrary plane domain. *CMES: Computer Modeling in Engineering & Sciences*, vol. 20, no. 2, pp. 111-122.

Liu, D.J; Yu, D. H.(2008): The coupling method of natural boundary element and mixed finite element for stationary Navier-Stokes equation in unbounded domains. *CMES: Computer Modeling in Engineering & Sciences*, vol. 37, no. 3, pp. 305-330.

Owatsiriwong, A.; Phansri, B.; Park, K.H. (2008): A cell-less BEM formulation for 2D and 3D elastoplastic problems using particular integrals. *CMES: Computer Modeling in Engineering & Sciences*, vol.31, no.1, pp. 37-59.

Prenter, P. M. (1975): *Splines and Variational Methods*. Wiley, New York.

Shiah, Y.C.; Tan, C.L. (2000): Fracture mechanics analysis in 2D anisotropic thermoelasticity using BEM, *CMES: Computer Modeling in Engineering & Sciences*, vol.1, no. 3, pp. 91-99.

Wang, H. T.; Yao, Z. H. (2005): A New Fast Multipole Boundary Element Method for Large Scale Analysis of Mechanical Properties in 3D Particle-Reinforced Composites. *CMES: Computer Modeling in Engineering & Sciences*, vol. 7, no. 1, pp. 85-96.

Wang, H. T.; Yao, Z. H. (2008): A Rigid-fiber-based Boundary Element Model for Strength Simulation of Carbon Nanotube Reinforced Composites. *CMES: Computer Modeling in Engineering & Sciences*, vol. 29, no. 1, pp. 1-14.

Wang, S.; Zhang, Y. (2004): Vibration Analysis of Rectangular Composite Laminated Plates Using Layerwise B-spline Finite Strip Method. *Composite structures,* 68, pp. 349-358.

Yuan, W. X.; Dawe, D. J. (2004): Free Vibration and Stability Analysis of Stiffened Sandwich Plates. *Composite Structures*, 63, pp. 123-137.

Zhang, Y. H.; Li, Q. S.; Lin, J. H.; Williams, F. W. (2009): Random Vibration Analysis of Long-span Structures Subjected to Spatially Varying Ground Motions. *Soil Dynamics and Earthquake Engineering*, 29, pp. 620-629.

Zhou, Y.T.; Li,X.; Yu, D. H.(2008): Integral method for contact problem of bonded plane material with arbitrary cracks., *CMES: Computer Modeling in Engineering & Sciences*, vol. 36, no.2, pp. 147-172.